JOURNAL OF MATERIALS SCIENCE 28 (1993) 5684–5692

A method for measuring temperature-dependent stress and thermal expansion of coatings

CHIN-CHEN CHIU
Department of Metallurgy, Mechanics, and Materials Science, Michigan State University, East Lansing, Michigan 48824, USA

Equations and a strain-gauge technique have been presented previously for the determination of the residual stresses in ceramic coatings. In the current work, the equations are rewritten in terms of simple form. The technique is extended to elevated-temperature environments. The stress–temperature relations of coated systems are modelled according to elastic and thermoviscoelastic theory. In addition, residual stress and thermal expansion coefficient measurements are performed on SiC coating–graphite substrate composites.

1. Introduction

Ceramic coatings as protective layers can improve the high-temperature corrosion resistance of substrates. For example, silicon carbide coatings are used to protect the carbon–carbon nose cap on the space shuttle from high-temperature oxidation [1]. ZrO_2-based coatings serve as thermal barriers in heat engines [2]. Because of the thermal expansion mismatch between the coatings and the substrates, residual stresses develop in the coatings [3, 4]. The stresses may cause microcracking or delamination of the coatings. Thus, the residual stress in coatings is a basic parameter for characterizing coating performance.

The room-temperature residual stresses in coatings can be determined using a strain-gauge technique [3]. However, when coated materials are required for high-temperature applications, the knowledge of stress–temperature relations becomes important for coating design. The influence of thermal history on residual stress development has been experimentally studied in recent years [5–16]. The residual stresses in as-deposited films are dependent on processing conditions [17–21]. After thermal annealing, the chemical, physical and microstructural properties of coatings become stable. Thus, the stress–temperature relations become regular and reproducible [9–12]. However, various coated materials still exhibit distinctive stress–temperature relations. Thus, a theoretical analysis is necessary to unify the experimental results. Grunling *et al.* [22] presented a stress–temperature relation model showing that the stresses in elastic coatings vary linearly with temperature. Flinn *et al.* [23] proposed an elastic–plastic deformation model indicating that plastic deformation causes the stress in aluminium films to form a temperature-dependent hysteresis loop. Some researchers [24–27] have proposed that viscoelasticity could cause silicate films to develop a time-dependent stress relaxation.

The purpose of this paper is (i) to rewrite the residual stress calculation formulae which have been presented previously in terms of simple form, (ii) to extend the strain-gauge technique for measuring the temperature-dependent stress and thermal expansion co-efficient of coating, and (iii) to propose stress–temperature relation models for coated materials.

2. Theoretical considerations

2.1. Stress determination of coating

Surface strains, induced by the separation of coatings and substrates, can be indices for determining the residual stresses in coatings [3]. When the coating layer in Fig. 1a is totally polished off, the substrate develops a strain. The surface strain ε_{s*} detected by the strain gauge can be used to calculate the average residual stress in coatings, σ^*:

$$\sigma^* = -\frac{E_s\varepsilon_{s*}R(E_sR^3 + E_c)}{2E_sR^3 + 3E_sR^2 - E_c} \quad (1)$$

where

$$R = l_s/l_c$$

The subscripts c and s refer to properties of the coating and the substrate, respectively. E and l are the elastic modulus and the thickness, respectively. Equation 1 is equivalent to Equation 18b of Chiu [3], as can be proved by substituting W into that equation. Similarly, when the substrate in Fig. 1b is totally polished off, a surface strain ε_{c*} arises in the coating. Thus

$$\sigma^* = -\frac{E_c\varepsilon_{c*}(E_sR^3 + E_c)}{E_sR^3 - 3E_cR - 2E_c} \quad (2)$$

Equations 1 and 2 have the same function for determining the average residual stress in coatings. The relationship between the material properties and σ^* can be described by

$$\sigma^* = \frac{E_c\Delta T(\alpha_c - \alpha_s)E_sR(E_sR^3 + E_c)}{4(E_sR^3 + E_c)(E_sR + E_c) - 3(E_sR^2 - E_c)^2} \quad (3)$$

where α is the thermal expansion coefficient. ΔT is the

0022–2461

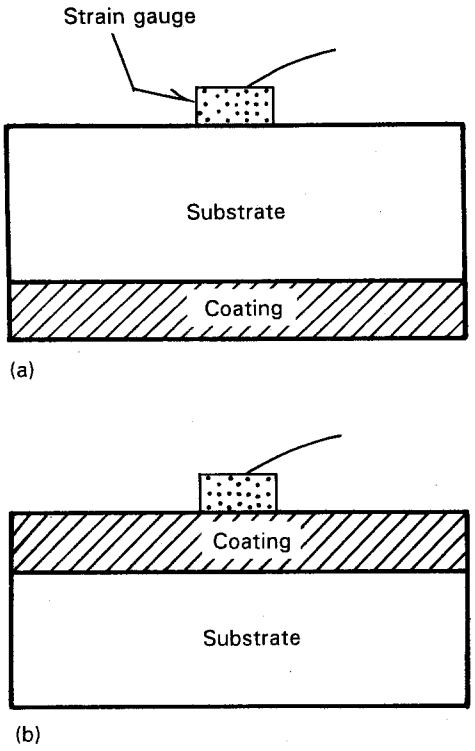

Figure 1 Schematic diagram of the strain-gauge set-up for measuring the surface strain on (a) the substrate and (b) the coating. The surface strains arise when the coating and substrate separate from each other.

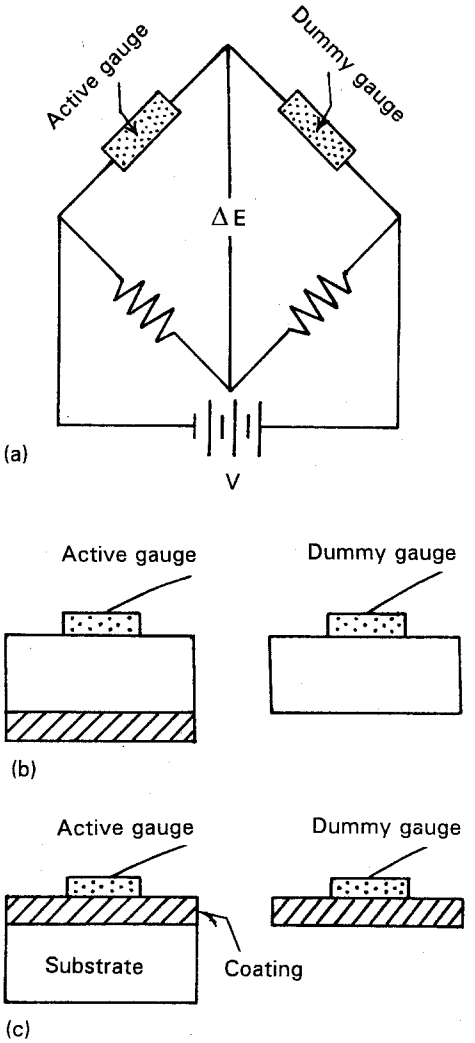

Figure 2 (a) Wheatstone bridge and strain-gauge circuits for elevated-temperature measurement. (b, c) Set-ups of the active gauge and the dummy gauge for measuring the coating's residual stress.

temperature difference between the fabrication temperature (or annealing temperature) and the room temperature (or the temperature T at which σ^* is measured). Following a similar argument as for Equation 1, Equations 2 and 3 are equivalent to Equations 18a and B-5, respectively, of Chiu [3].

The saturation stress, $E_c\Delta T(\alpha_c - \alpha_s)$, has to be known in advance before the use of Equation 3. Combining Equations 1 and 3 gives

$$\sigma_{sat} = E_c\Delta T(\alpha_c - \alpha_s) = -\frac{\varepsilon_{s^*}[4(E_sR^3 + E_c)(E_sR + E_c) - 3(E_sR^2 - E_c)^2]}{2E_sR^3 + 3E_sR^2 - E_c} \quad (4a)$$

Equation 4a is a formula for determining σ_{sat} from ε_{s^*}. σ_{sat} can also be determined from ε_{c^*} using the following equation, deduced from the combination of Equations 2 and 3:

$$\sigma_{sat} = E_c\Delta T(\alpha_c - \alpha_s) = -\frac{\varepsilon_{c^*}E_c[4(E_sR^3 + E_c)(E_sR + E_c) - 3(E_sR^2 - E_c)^2]}{E_sR(E_sR^3 - 3E_cR - 2E_c)} \quad (4b)$$

σ_{sat} is a constant for coated systems with the same coating and substrate materials. Thus, σ_{sat} is a parameter for coated materials.

2.2. Strain-gauge circuits for elevated-temperature measurement

When a strain gauge is used for elevated-temperature measurement, the temperature-induced change in the gauge's electric resistance has to be considered. Temperature compensation can be achieved through a Wheatstone bridge circuit with an active gauge and a dummy gauge (Fig. 2a) [28].

In the case of measuring the residual stresses in coatings, the set-up of the active gauge and the dummy gauge is illustrated in Fig. 2b. The active gauge is attached to the uncoated surface of the substrate. The dummy gauge is attached to a monolithic substrate (without coating). When the gauges are placed together in a furnace, the temperature-induced changes in the gauge's electric resistance are cancelled out in the Wheatstone bridge circuit (Fig. 2a and b). The observed temperature-dependent strain, ε_0, is associated with the relative change in the coating's residual stresses, with respect to a reference temperature.

In general, the gauge factor is set for room-temperature measurement (regarding room temperature as a reference temperature) and then ε_0 is continuously observed without changing the gauge factor. Thus, ε_0 has to be transformed into the real strain ε which corresponds to the real gauge factor at a given measurement temperature. The output voltage, ΔE, of

the Wheatstone bridge is [28]

$$\Delta E = \frac{R_1 + R_2}{(R_1 + R_2)^2} V(G_0 \varepsilon_0) \quad (5)$$

where R_1 and R_2 are the electric resistance of the active gauge and the dummy gauge, respectively. V and G_0 are the bridge voltage and the gauge factor at room temperature, respectively. Since ΔE, R_1, R_2 and V are constants at a given measurement temperature, Equation 5 yields

$$\varepsilon = \frac{G_0}{G} \varepsilon_0 \quad (6)$$

where G is the real gauge factor at the measurement temperature. Calculating the real strain using Equation 6 and then substituting the real strain into Equation 1 (replacing ε_{s*} by ε), we obtain the relative change in the coating's residual stress, $\Delta\sigma^*$. The sum of $\Delta\sigma^*$ and σ^* (σ^* = room-temperature residual stresses) gives the stress–temperature relation.

After the measurement of $\Delta\sigma^*$, the linear thermal expansion coefficient of the coating can accordingly be evaluated. Assume that E_c, E_s and $(\alpha_c - \alpha_s)$ are independent of temperature. Differentiating Equation 3 with respect to T yields

$$\frac{d\sigma^*}{dT} = -(\alpha_c - \alpha_s) \times \frac{E_c E_s R(E_s R^3 + E_c)}{4(E_s R^3 + E_c)(E_s R + E_c) - 3(E_s R^2 - E_c)^2} \quad (7)$$

Thus, the slope of the stress–temperature curve, $d\sigma^*/dT$, is proportional to $(\alpha_c - \alpha_s)$. Once the thermal expansion coefficient of the substrate α_s is known, α_c can be calculated using Equation 7.

The temperature-dependent stress in the coating can also be measured using another set-up of the strain-gauge circuit (Fig. 2c). The active gauge is attached to the coated surface of the substrate. The dummy gauge is attached to a monolithic coating layer (without substrate). The measurement procedures and real strain calculation are the same as those described above, except that the real strain is substituted into Equation 2 (replacing ε_{c*} by ε) to calculate $\Delta\sigma^*$. The sum of $\Delta\sigma^*$ and σ^* yields the stress–temperature relation. Similarly, α_c can be evaluated from Equation 7.

2.3. Stress–temperature relation models

The residual stresses in as-deposited coatings are functions of coating conditions [17–21]. Before thermal stabilization, the as-deposited coatings may have intrinsic volume dilatation (or shrinkage) in comparison with the annealed coatings. The difference in volume can be attributed to point defects, disordered crystallization, trapped gas, metastable phases, glassy phase, etc. [17–21], which induce intrinsic strain ε_i (intrinsic stress) in the coatings. After thermal stabilization at the annealing temperature T_a, the intrinsic strain is relieved and the material properties of the coating become stable. In general, coated materials are elastic in the temperature range of $T < T_a$. At $T > T_a$, the coated materials can be viscoelastic because of the glassy phase involved in ceramic coatings (or ceramic substrates). This section presents stress–temperature relation models for coated systems (a) with thermal stabilization, (b) without thermal stabilization, and (c) with thermoviscoelastic properties.

2.3.1. After thermal stabilization

After thermal stabilization at $T \approx T_a$, the residual stresses in coatings are only attributed to the thermal

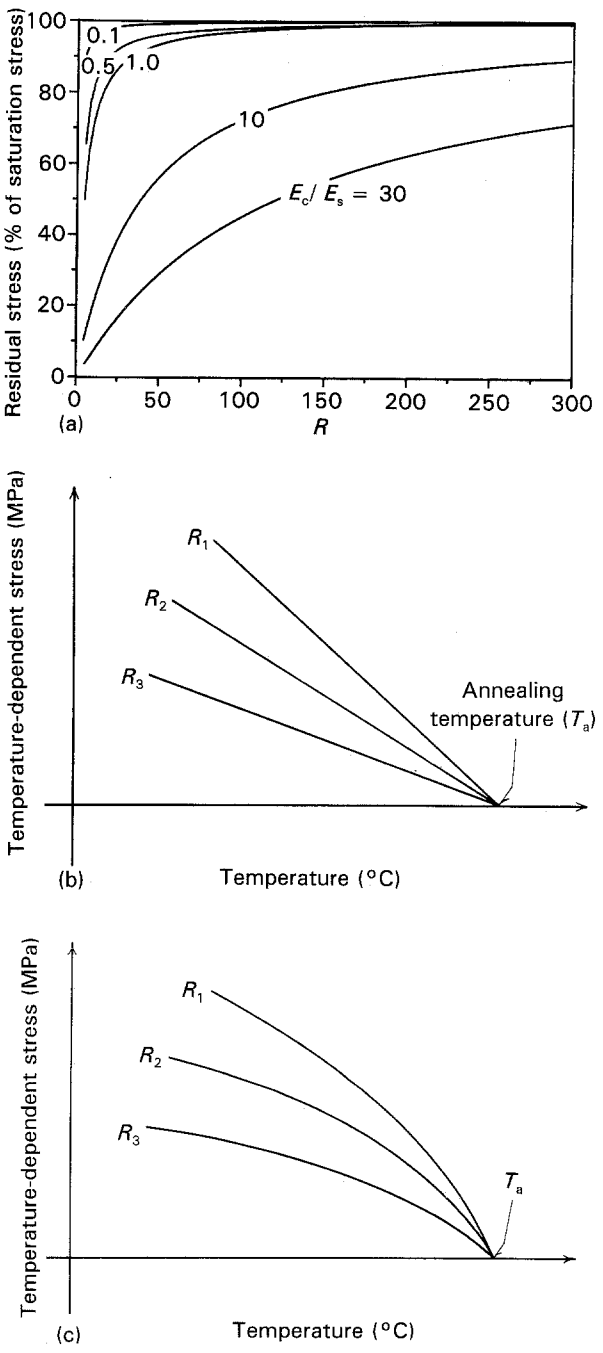

Figure 3 Elastic stress–temperature relation models, neglecting intrinsic strain effects. (a) Variation of the coating's room-temperature residual stress with the ratio of substrate thickness to coating thickness, R. (b) Variation of the coating's residual stress with temperature, where the material properties are assumed to be independent of temperature; $R_1 > R_2 > R_3$. (c) Stress–temperature relations, where the material properties are assumed to be temperature-dependent.

expansion mismatch between the coating and the substrate. For linearly elastic coated systems, the room-temperature stresses increase as R increases (Equation 3 and Fig. 3a). In this paper, the coated material is assumed to have a uniform temperature change, without a temperature gradient in the material. Thus, if $(\alpha_c - \alpha_s)$, E_c and E_s are independent of temperature, the stresses linearly decrease with temperature increase and various R values correspond to individual stress–temperature curves (Equation 3 and Fig. 3b). The intersection of a curve and the abscissa is the annealing temperature of the coated material, T_a, which is unique for coated systems with the same coating and substrate materials. If $(\alpha_c - \alpha_s)$, E_c and E_s are temperature-dependent, the term $\Delta T(\alpha_c - \alpha_s)$ in Equation 3 has to be rewritten as

$$\int_T^{T_a} (\alpha_c - \alpha_s) \mathrm{d}T \tag{8}$$

The stress–temperature relations become non-linear (Fig. 3c). However, the coated system still have a unique T_a. Since the coated systems are elastic, the stress–temperature relations in Fig. 3b and c are reversible in thermal cycling. Some investigators [8–10] have reported experimental results which agree with the elastic model.

2.3.2. Before thermal stabilization

Before thermal stabilization, the temperature-dependent stress has to be analysed according to the superposition of the intrinsic strain ε_i and the thermal expansion-induced strain $\Delta T(\alpha_c - \alpha_s)$ (Appendix A). The stress–temperature curves in Fig. 3b will be shifted, depending on the characteristics of the intrinsic strain. If ε_i and $\Delta T(\alpha_c - \alpha_s)$ have different signs (for example, one is positive and the other negative), the intrinsic strain offsets the thermal expansion-induced strain. Thus, the as-deposited coatings have a smaller residual stress (solid line in Fig. 4a) than the annealed coatings (dashed line). If not, the residual stress in as-deposited coatings becomes greater (Fig. 4b). If the as-deposited coatings have the same E_c as the annealed coatings, the solid line is parallel to the dashed line. When the as-deposited coatings are repeatedly tested in the temperature range of $T \ll T_a$, the temperature-dependent stress reversibly follows the solid line [5–7]. However, the intrinsic strain can be relieved* during thermal testing in which the temperature is up to $T \simeq T_a$. Thus, the dotted curve develops at $T \simeq T_a$ (Fig. 4a and b) connecting the solid line and dashed line. These curves form a U-shaped stress–temperature relation. Once the as-deposited coatings are "thermally stabilized" in the first cycle, the stress–temperature relations will follow the dashed line (annealed coatings) in further thermal cycling [9–12].

In contrast to strain relaxation, the intrinsic strain may deteriorate during thermal cycling, which results from coating oxidation or coating–substrate interaction [29, 30]. Thus, the solid lines in Fig. 4a and b will further deviate from the dashed line. Finally, the coating's residual stress may become great enough to cause microcracking or delamination [29].

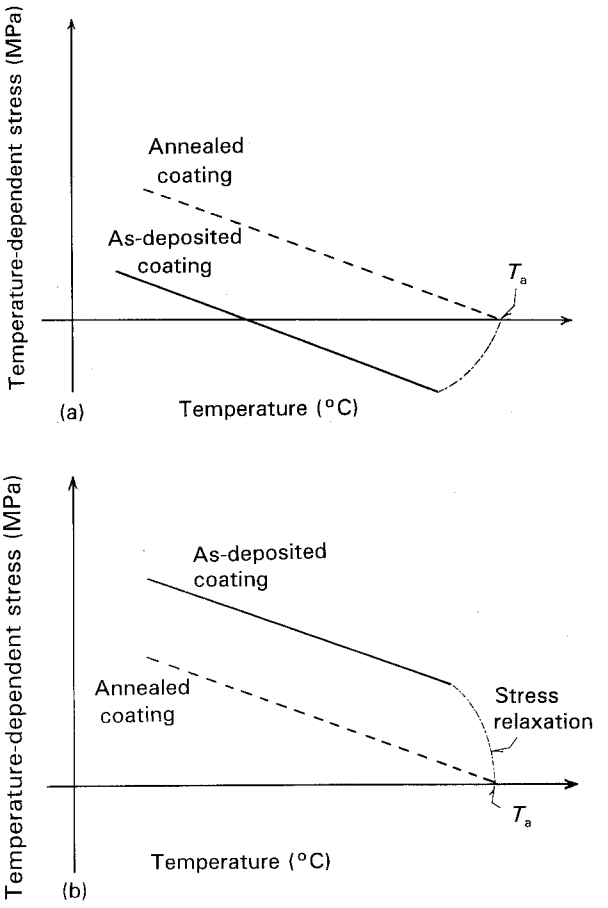

Figure 4 Elastic stress–temperature relation models, taking into account intrinsic strain effects. (a) The intrinsic strain effects decrease the coating's residual stress, shifting the stress–temperature curve from the dashed line (annealed coating) to the solid line (as-deposited coating). (b) The intrinsic strain effects increase the coating's stress.

2.3.3. Thermoviscoelastic property involved

Coated materials can be viscoelastic when they serve in thermal environments involving the temperature ranges of $T < T_a$ and $T > T_a$. In this section, $(\alpha_c - \alpha_s)$, E_c and E_s are assumed to be independent of temperature, as well as the coating layer having the same material properties as window glass (see Appendix B). Fig. 5 illustrates the numerical results showing the effect of thermoviscoelasticity on the coating's stress. In the initial stage of the thermal cycling (point A), the stress linearly changes as temperature increases (Fig. 5a). When $T \geq 580\,^\circ\mathrm{C}$ (point B), stress relaxation occurs. At $T \simeq 630\,^\circ\mathrm{C}$ (point C), the stress curve enters a thermoviscoelastic hysteresis loop (Fig. 5a and b). From then on, the development of the temperature-dependent stress follows the arrow in further thermal cycling. It is apparent that the temperature-dependent stress in the first cycle forms a U-shaped curve (see also Fig. 4a).

* Stress relaxation may be achieved by the evolution of trapped gas, recrystallization of metastable phases, plastic deformation, viscous flow, etc. The viscous flow-induced stress relaxation is discussed in Appendix B.

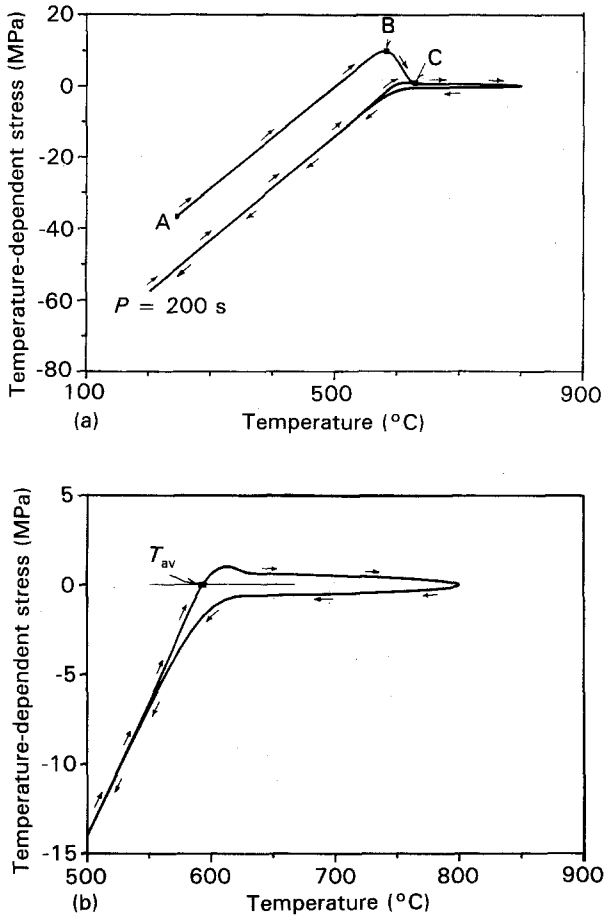

Figure 5 Thermoviscoelastic stress–temperature relation models. (a) Temperature-dependent stress in the coating, in which the stress curve develops a thermoviscoelastic hysteresis loop. (b) Enlargement of the hysteresis loop. T_{va} is the observed annealing temperature at which the coating's stress is zero.

Thermoviscoelasticity results in stress relaxation and/or quench-induced stress [31, 32], so that the stress in a coating is a function of the temperature change rate and thermal history. The magnitude of the stress at a given temperature increases with a decrease of the thermal cycling period, P, in comparison with the dashed line (annealed coating layer) in Fig. 6. In addition, the observed annealing temperature shifts from T_a to T_{av}. Shintani *et al.* [16] proposed that

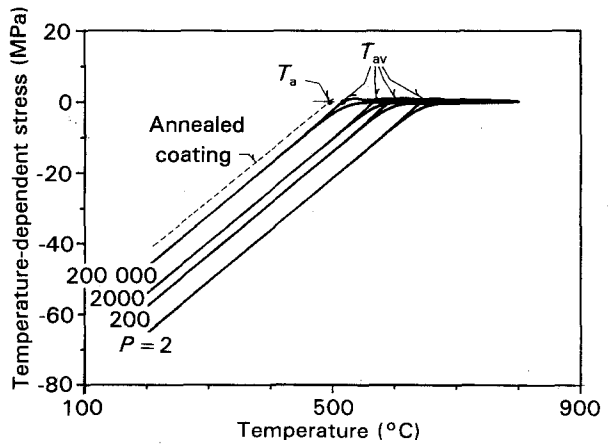

Figure 6 Influence of the thermal cycling period, P, on the temperature-dependent stress. When P approaches infinity the stress curve converges to the dashed line (annealed coating layer).

viscoelasticity could cause silicate films to develop a time–temperature-dependent stress relaxation. Since Shintani *et al.* only performed one cycle of stress–temperature testing, they presented the U-shaped stress–temperature relation (stress relaxation phenomenon), rather than the hysteresis loop predicted in Figs 5 and 6.

The main differences between elastic models and thermoviscoelastic models are as follows:

(i) The elastic models give reversible stress–temperature relations which are independent of the time–temperature path (Fig. 3b and c).

(ii) Elastic models are applied to the temperature range of $T < T_a$ and thermoviscoelastic models become involved in the temperature ranges of $T < T_a$ and $T > T_a$.

(iii) Thermoviscoelastic models yield a stress–temperature hysteresis which is a function of thermal history (Figs 5 and 6).

(iv) Thermoviscoelasticity can increase the coating's stress so that the stress-induced damage could be underestimated according to the observed room-temperature stress in the annealed coating.

3. Experimental procedure

Chemical vapour-deposited SiC coating–graphite substrate composites were used in these experiments. The as-received billets (Material Technology Corporation, Dallas, TX, USA) were annealed in an electric furnace in a nitrogen atmosphere at 1100 °C for 2 h. The cooling rate was 2 °C min^{-1}. Using a low-speed diamond saw, the annealed billets were cut into specimens 8 cm × 0.8 cm × 0.5 cm, with coating on a single 8 cm × 0.8 cm surface. The uncoated surfaces of graphite substrate were polished using 600 grit SiC polishing papers. The specimen thickness was determined to within ± 0.002 cm using a micrometer and the coating thickness was measured using an optical microscope. To obtain monolithic SiC coating layers (without graphite substrate), some as-deposited and annealed composite specimens were heated in an electrical furnace in air at 550 °C until the graphite was totally oxidized.

To measure the room-temperature residual stress of coatings, a strain gauge (EA-06-125BZ-350, Measurement Group Inc., Raleigh, NC, USA) was attached to the coated surface of the specimen, parallel to the beam axis. When the graphite substrate was polished off, a surface strain ε_c was detected by the strain gauge (see Fig. 1b). The coating's residual stresses, σ^* and σ_{sat}, were calculated using Equations 2 and 4b, respectively.

The temperature-dependent stresses in SiC coatings were measured according to the strain-gauge set-up shown in Fig. 2c. If the annealed composite specimen was tested, the dummy gauge was attached to the annealed monolithic SiC coating layer. If the as-deposited specimen were tested, the dummy gauge was attached to the as-deposited monolithic SiC coating layer. The thermal expansion coefficient of the coating was evaluated using Equation 7.

Using a standing wave resonance method [33], the elastic moduli of SiC coatings were measured via the SiC coating–graphite composite specimens. The resonance frequencies of the composite specimens were measured before and after thermal annealing at 1100 °C. The measurement technique and the modulus calculation equations were described elsewhere [33]. The modulus of a monolithic graphite specimen 8.57 cm × 0.805 cm × 0.285 cm (without coating) was also measured using the resonance method [33].

4. Results and discussion

Observation by optical microscopy showed that the thickness of SiC coatings ranged from 89 to 103 μm. The elastic moduli of SiC coatings were measured using a standing-wave resonance method via the SiC coated graphite specimens [33]. The data populations give somewhat different mean values for the SiC coatings before and after thermal annealing (Table I). To test whether the two data populations are statistically identical, the (two-sided) Mann–Whitney U test is adopted. At a significance level $\alpha = 0.05$, the analysis indicates that there is not sufficient evidence to indicate a difference in the two data populations. This means that thermal annealing at 1100 °C does not cause a change in the elastic modulus of the SiC coating. The elastic modulus of a monolithic graphite specimen was 10.0 GPa, which was measured using the resonance method [33]. In the present study, $E_c = 371.7$ GPa and $E_s = 10.0$ GPa were adopted to calculate the residual stresses in SiC coatings.

The residual stresses in SiC coatings are compressive, since the separation of the SiC coating and the graphite substrate causes a positive surface strain ε_{c^*}. Fig. 7 illustrates the variation of the room-temperature average stress, σ^*, with respect to the ratio of the substrate thickness to the coating thickness, R. The solid curve and the dashed curve [3] represent the annealed and the as-received specimens, respectively. The stress increases as R increases, which agrees with the theoretical analysis shown in Fig. 3a. Thermal stabilization decreases σ^*, shifting from the dashed curve to the solid curve. Furthermore, thermal stabilization decreases the saturation stress σ_{sat} from 785 to 403 MPa. Thus, it is apparent that thermal annealing at 1100 °C can cause the intrinsic strain relaxation of as-received SiC coatings. However, more work is required to study the reason why thermal annealing decreases the residual stresses in SiC coatings without affecting the coating's elastic modulus.

TABLE I Influence of thermal annealing at 1100 °C on the elastic moduli of SiC coatings

Elastic modulus (GPa)			
Before stabilization		After stabilization	
407.5	433.6	372.0	365.1
378.3	411.0	394.6	349.0
294.8	369.0	317.4	407.3
387.2	340.4	420.9	329.2
377.4	395.7	381.3	380.4
Mean = 379 ± 39.2		Mean = 371.7 ± 31.1	

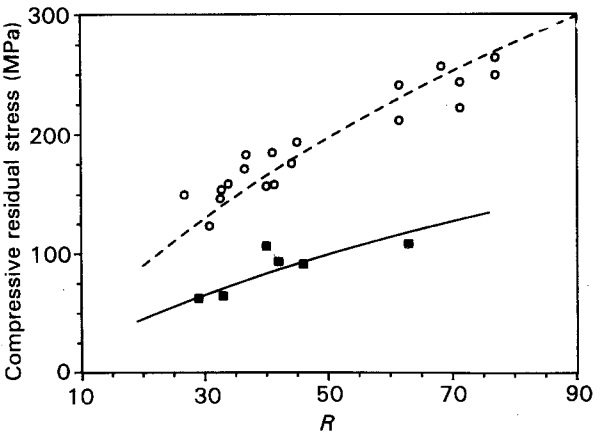

Figure 7 Room-temperature residual stresses in SiC coatings, as a function of the ratio of substrate thickness to coating thickness, R. The regression curves were calculated using Equation 3. (○) As received, (■) annealed.

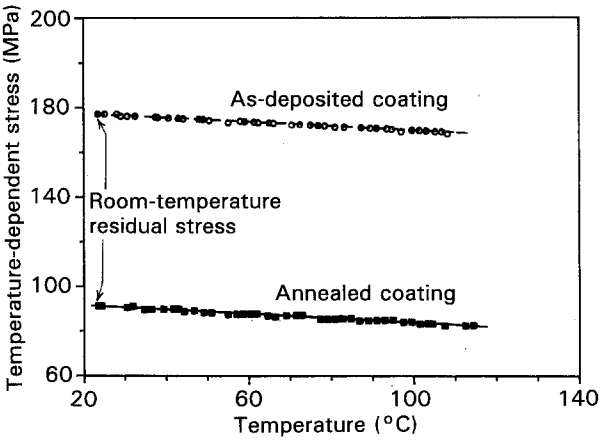

Figure 8 Variation of the residual stress in an SiC coating with respect to temperature. The thickness ratio of the tested specimen is $R = 46$. The room-temperature residual stresses were calculated according to the regression curves shown in Fig. 7.

Fig. 8 shows the temperature-dependent stress in SiC coatings. The solid and dashed lines, which are calculated using the least-squares method, represent the annealed and the as-received specimens, respectively. Thermal stabilization results in a shift from the dashed line to the solid line. The stress decreases linearly with temperature increase, implying that the material properties of SiC-coated graphite (such as E_c, E_s and $(\alpha_c - \alpha_s)$) are not sensitive to a temperature fluctuation from 23 to 110 °C (see Equation 3 and Fig. 4b). Since the strain gauges used can only operate from −75 to +175 °C, the present study fails to show whether or not thermoviscoelastic hysteresis exists in SiC-coated graphite. If the intersection of solid lines and the abscissa is evaluated with the help of extrapolation, a solution of $T \simeq 970$ °C is obtained. Thus, the annealing temperature of SiC-coated graphite could be 970 °C.

The slope of the solid line in Fig. 8 is -0.0961×10^6 Pa °C^{-1}. Based on Equation 7, the magnitude of

$(\alpha_c - \alpha_s)$ is calculated to be $-1.12 \times 10^{-6}\,°C^{-1}$. If the thermal expansion coefficient of the substrate, α_s, is known, then α_c can be evaluated.

5. Summary

A strain-gauge technique can determine the room-temperature residual stresses in coatings. In this paper, the technique is extended to measure the temperature-dependent stress. The technique is useful in measuring the linear thermal expansion coefficient of coatings.

This paper has proposed elastic and thermoviscoelastic models for analysing the variation of a coating's stress with temperature. If coated materials experience thermal cycling below the annealing temperature ($T < T_a$), the materials are elastic and the temperature-dependent stress is reversible (Fig. 3). If the coated materials serve in thermal environments involving the temperature ranges of $T < T_a$ and $T > T_a$, the materials can be viscoelastic. Thus, the temperature-dependent stress will be characterized by a thermoviscoelastic hysteresis loop which is a function of thermal history (Figs 5 and 6).

Experimental results on SiC coating–graphite composites indicate that the residual stresses in coatings decrease linearly as the temperature increases from 23 to 110 °C. Thermal stabilization decreases the coating's residual stresses from $\sigma_{sat} = 785$ MPa to $\sigma_{sat} = 403$ MPa. However, a statistical analysis of the (two-sided) Mann–Whitney U test showed no statistically significant change in the elastic moduli of SiC coatings before and after thermal stabilization. Since the operating temperature of the strain gauges used for stress measurement is limited to $-75\,°C < T < 175\,°C$, the present study fails to show whether or not the coated materials exhibit a thermoviscoelastic hysteresis loop at high temperature.

Appendix A: Effect of thermal expansion mismatch

The thermal expansion mismatch between the coating and the substrate causes the residual stresses in coatings. As shown in Equation (B-1) of Chiu [3], the thermal expansion-induced strain $\Delta T(\alpha_c - \alpha_s)$ is involved in the mathematical derivation of the coating's residual stress by means of the equation

$$\Delta T(\alpha_c - \alpha_s) = \varepsilon_{cl} - \varepsilon_{sl} \quad \text{(A1)}$$

where ε_{cl} and ε_{sl} are the axial strain in the coating and in the substrate, respectively [3]. Equation A1 is only suitable for coated materials which have been thermally stabilized. To take into account the intrinsic strain in coatings, ε_i, Equation A1 should be rewritten according to the superposition principle, namely

$$\Delta T(\alpha_c - \alpha_s) + \varepsilon_i = \varepsilon_{cl} - \varepsilon_{sl} \quad \text{(A2)}$$

The mathematical derivation procedures for evaluating coating's stress are the same as those given elsewhere [3]. The consequent results yield equations similar in form to Equations 1–4, except that the term $\Delta T(\alpha_c - \alpha_s)$ in Equations 3 and 4 is replaced by $\Delta T(\alpha_c - \alpha_s) + \varepsilon_i$. Since ε_i is a constant, Equation 7 is still valid for calculating the thermal expansion coefficient of the coating.

Appendix B: Effect of thermoviscoelasticity on the coating's residual stresses

Ceramic coatings (or ceramic substrates) may contain a glassy phase. Thus, the coated systems can behave as viscoelastic materials at elevated temperature, and the stress–temperature relations are dependent on thermal history. The effect of viscoelasticity on temperature-dependent stress have been reported by some researchers [24–27]. However, those studies focus on the constant-temperature state. In this appendix, we treat the coatings as linearly viscoelastic materials (Maxwell solids) and analyse the stress–temperature relations in a non-constant temperature state (thermal cycling conditions).

In the temperature range of $T < T_a$, the coated systems are linearly elastic materials so that the residual stress distributions in the coatings and in the substrate are individually linear functions of the Z coordinate in Fig. B1b. The average residual stress, σ^*, in coatings develops as described by Equation 3. In terms of a simple form, we have

$$\sigma^* = E_c \varepsilon^* \quad \text{(B1)}$$

where

$$\varepsilon^* = (T_a - T)(\alpha_c - \alpha_s) M \quad \text{(B2)}$$

$$M = \frac{E_s R(E_s R^3 + E_c)}{4(E_s R^3 + E_c)(E_s R + E_c) - 3(E_s R^2 - E_c)^2} \quad \text{(B3)}$$

ε^* is defined as an average strain in coatings. If $(\alpha_c - \alpha_s)$, E_s and E_c are independent of temperature, the temperature fluctuation-induced strain is

$$\frac{d\varepsilon^*}{dT} = -M(\alpha_c - \alpha_s) \quad \text{(B4)}$$

By means of proposing an average strain, the two-dimensional elastic problem of the coating's residual stress can be considered as a one-dimensional problem. This means that σ^* changes linearly with $d\varepsilon^*$.

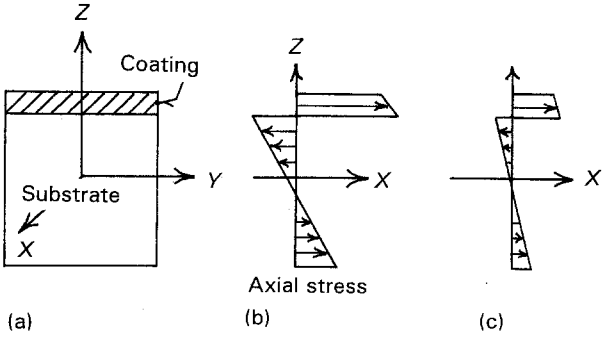

Figure B1 (a) Cross-section of coated specimen. (b) Residual stress distribution in a linearly elastic specimen, (c) Transient stress distribution in a viscoelastic specimen after an elapsed time.

In the temperature range of $T > T_a$, the coating's stress is a two-dimensional thermoviscoelastic problem (variables: position, time and temperature). The stress relaxation of linearly viscoelastic materials under isothermal conditions is [32]

$$\sigma(t) = \sigma_0 \exp\left(\frac{t}{\tau_0}\right) \quad \text{(B5)}$$

where σ_0, $\sigma(t)$, τ_0 and t are the instantaneous stress, time-dependent stress, relaxation time, and time, respectively. According to the analysis of stress relaxation (Equation B5) and stress redistribution, the stress distributions in the coatings and in the substrate are still individually linear functions of Z after a certain elapsed time (Fig. B1c). If $(\alpha_c - \alpha_s)$, E_s and E_c are independent of temperature, the strain–temperature relation of Equation B4 is still valid for linearly viscoelastic materials. (Similar arguments of strain–temperature relations are used in Equations 6, 5.102 and 40 of references 31, 32 and 34, respectively.) Thus, the thermoviscoelastic problem can be simplified to a one-dimensional problem (variables: time and temperature). The development of σ^* is equivalent to the stress relaxation of a Maxwell solid which is continuously subjected to a temperature fluctuation-induced strain, $d\varepsilon^*$. The accompanying restrictions are that (i) E_s, E_c and $(\alpha_c - \alpha_s)$ are constants, and (ii) the coated materials are subjected to a uniform temperature change with respect to time, without a spatial temperature gradient.

The one-dimensional isothermal stress–strain relation of linearly viscoelastic materials is [32]

$$\sigma(t) = \int_0^t E(t - t') \frac{\partial \varepsilon(t')}{\partial t'} dt' \quad \text{(B6)}$$

where $E(t)$, σ, and ε are the relaxation modulus, stress and strain, respectively. If there is an initial stress loading σ_i at $t = 0$, then

$$\sigma(t) = \sigma_i E(t) + \int_0^t E(t - t') \frac{\partial \varepsilon(t')}{\partial t'} dt' \quad \text{(B7)}$$

To couple the temperature variation effect [31, 32], t is replaced by the reduced time ξ, such that

$$\sigma(\xi) = \sigma_i E(\xi) + \int_0^\xi E(\xi - \xi') \frac{\partial \varepsilon(\xi')}{\partial \xi'} d\xi' \quad \text{(B8)}$$

where

$$\xi(t) = \int_0^t \Phi[T(t')]\, dt' \quad \text{(B9)}$$

$T(t)$ and Φ are the time-dependent temperature and the shift function of the viscoelastic material, respectively [31, 32]. The chain rule gives

$$\frac{d\varepsilon}{d\xi} = \left(\frac{d\varepsilon}{dT}\right)\left(\frac{dT}{d\xi}\right) \quad \text{(B10)}$$

Combining Equations B4, B8 and B10 yields

$$\sigma^*(\xi) = \sigma_i E(\xi) - M(\alpha_c - \alpha_s) \int_0^\xi E(\xi - \xi') \frac{dT(\xi')}{d\xi'} d\xi' \quad \text{(B11)}$$

TABLE B1 Numerical values in calculations of the temperature-dependent stress in coatings

Thermal expansion difference $(\alpha_c - \alpha_s)$	$3 \times 10^{-6}\,°C^{-1}$
Elastic modulus of coating (E_c)	70 GPa
Elastic modulus of substrate (E_s)	10 GPa
Period of thermal cycling (P)	200 s
Thickness ratio (R)	50

To refer to the physical time t, Equation B11 is rewritten as

$$\sigma^*(t) = \sigma_i E(\xi(t)) - M(\alpha_c - \alpha_s) \times \int_0^t E(\xi(t) - \xi(t')) \frac{dT(t')}{dt'} dt' \quad \text{(B12)}$$

where $\sigma^*(t)$ is the average stress in the coating as a function of thermal history. $\sigma^*(t)$ can be calculated using Equation B12 if the material parameters and thermal cycling conditions are given.

In order to numerically simulate the temperature-dependent stress, we assume that the coatings have the same material properties as window glass. The shift function of window glass measured at a base temperature of 538 °C is [31]

$$\log_{10}[\Phi(T)] = 0.03861(T - 538) \quad \text{(B13)}$$

The relaxation modulus in axial tension is [31, 35]

$$E(t) = E_c[0.43 \exp(-t/141) + 0.67 \exp(-t/756)] \quad \text{(B14)}$$

A periodic function can be rewritten in terms of trigonometric series (Fourier series). For convenience, the time-dependent temperature of coated systems is assumed to be

$$T(t) = 500 + 300 \sin(2\pi t/P) \quad \text{(B15)}$$

where P is the period of thermal cycling. In the numerical calculation, we first solve for $\xi(t)$ by combining Equations B9, B13 and B15. $\xi(t)$ is then stored. Equation B12 is simplified by combining with Equations B14 and B15, and is then integrated using the trapezoidal rule. Table B1 lists the required input values for the numerical analysis. Figs 5 and 6 illustrate the numerical results. The thermoviscoelastic model assumes that the coating is viscoelastic and the substrate is elastic. However, the physical meaning in Figs 5 and 6 is still valid for coated systems which consist of an elastic coating and a viscoelastic substrate.

Acknowledgements

The author would like to acknowledge Michael B. Miller (Material Technology Corporation, Dallas, TX), who provided SiC coating–graphite substrate composites.

References

1. W. L. VAUGHN and H. G. MAAHS, *J. Amer. Ceram. Soc.* **73** (1990) 1540.
2. J. W. WATSON and S. R. LEVINE, *Thin Solid Films* **119** (1984) 185.

3. C. C. CHIU, *J. Amer. Ceram. Soc.* **73** (1990) 1999.
4. R. W. HAFFMAN, *Mater. Sci. Eng.* **53** (1982) 37.
5. C. BLAAUW, *J. Appl. Phys.* **54** (1983) 5064.
6. D. S. WILLIAMS, *ibid.* **57** (1985) 2340.
7. A. K. SINHA, H. J. LEVINSTEIN and T. E. SMITH, *ibid.* **49** (1978) 2423.
8. M. SHIMBO, M. OCHI and K. ARAI, *J. Paint Technol.* **56** (1984) 45.
9. J. T. PAN and I. BLECH, *J. Appl. Phys.* **55** (1984) 2874.
10. D. M. MATTOX, in "Deposition Technologies for Films and Coatings", edited by R. F. Bunshah (Noyes, Park Ridge, New Jersey, 1982) p. 63.
11. M. SHIMBO and T. MATSUO, *J. Electrochem. Soc.* **130** (1983) 135.
12. S. T. CHEN, C. H. YANG, F. FAUPEL and P. S. HO, *J. Appl. Phys.* **64** (1988) 6690.
13. G. SMOLINSKY and T. P. H. F. WENDLING, *J. Electrochem. Soc.* **132** (1985) 950.
14. A. LAHAV and K. A. GRIM, *J. Appl. Phys.* **67** (1990) 734.
15. C. GOLDSMITH, P. GELDERMANS, F. BEDETTI and G. A. WALKER, *J. Vac. Sci. Technol.* **A1** (1983) 407.
16. A. SHINTANI, S. SUGAKI and H. NAKASHIMA, *J. Appl. Phys.* **51** (1980) 4197.
17. H. OIKAWA and Y. NAKAJIMA, *J. Vac. Sci. Technol.* **14** (1977) 1153.
18. M. YAMADA, M. NAKAISHI and K. SUGUSHIMA, *J. Electrochem. Soc.* **137** (1990) 2242.
19. M. S. CHOI and E. W. HEARN, *ibid.* **131** (1984) 2443.
20. R. LATHLAEN and D. A. DIEHL, *ibid.* **116** (1969) 620.
21. J. A. THORNTON and D. W. HOFFMAN, *J. Vac. Sci. Technol.* **14** (1977) 164.
22. H. W. GRUNLING, K. SCHNEIDER and L. SINGHEISER, *Mater. Sci. Eng.* **88** (1987) 177.
23. P. A. FLINN, D. S. GARDNER and W. D. NIX, *IEEE Trans. Electr. Dev.* **ED-34** (1987) 689.
24. G. C. RODA, F. SANTARELLI and G. C. SARTI, *J. Electrochem. Soc.* **8** (1985) 1909.
25. A. FARGEIX and G. GHIBAUDO, *J. Appl. Phys.* **54** (1983) 7153.
26. C. H. HSUEH and A. G. EVANS, *ibid.* **54** (1983) 6672.
27. E. A. IRENE, *ibid.* **54** (1983) 5416.
28. J. W. DALLY and W. F. RILEY, in "Experimental Stress Analysis" (McGraw-Hill, New York, 1978) p. 217.
29. R. A. MILLER, *J. Amer. Ceram. Soc.* **67** (1984) 517.
30. D. M. MATTOX, J. E. GREENE, D. H. BUCKLEY and G. A. SOMORJAI, *Mater. Sci. Eng.* **70** (1985) 79.
31. E. H. LEE, T. G. ROGERS and T. C. WOO, *J. Amer. Ceram. Soc.* **48** (1965) 480.
32. R. M. CHRISTENSEN, "Theory of Viscoelasticity' (Academic, New York, 1982) p. 77.
33. C. C. CHIU and E. D. CASE, *Mater. Sci. Eng.* **A132** (1991) 39.
34. R. MUKI and E. STERNBERG, *J. Appl. Mech.* **28** (1961) 193.
35. R. GARDON and O. S. NARAYANASWAMY, *J. Amer. Ceram. Soc.* **53** (1970) 387.
36. H. R. NEAVE and P. L. WORTHINGTON, in "Distribution-Free Tests" (Unwin Hyman, Winchester, MA, 1988) p. 109.

Received 29 May 1991
and accepted 17 November 1992